Advanced Research Center for Beam Science – Particle Beam Science –

http://wwwal.kuicr.kyoto-u.ac.jp/www/index-e.htmlx

Assoc Prof
IWASHITA, Yoshihisa
(D Sc)

Techn Staff
TONGU, Hiromu

Researcher (pt)

KATAYAMA, Ryo (D Sc)

Lect (pt)

HIROTA, Katsuya (D Sc) Osaka University

Students

DENG, Weichao (M2)
TAKEUCHI, Yusuke (M2)
YAMAZAKI, Yuki (M2)
ABE, Masashi (M1)
YAKO, Tomoki (M1)

Scope of Research

We are studying particle beam science which includes particle beam generation, acceleration and manipulation for fundamental sciences as well as for practical applications, such as new materials and cancer therapy. We also concentrate on electromagnetics design such as Neutron Optics, including neutron beam focusing to highly enhance their efficiency for advanced measurements. We are the first in the world to demonstrate active neutron acceleration in order to seek the neutron Electric Dipole Moment. In addition, we contribute to advanced fault detection techniques for the International Linear Collider project superconducting accelerating cavities.

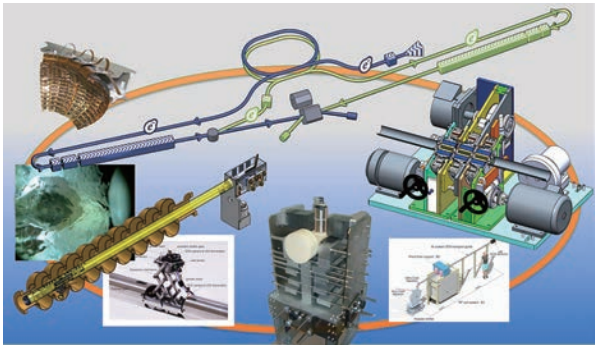

KEYWORDS

Beam Physics
Accelerator Physics
Neutron Optics
Phase Rotation
International Linear Collider

Selected Publications

Iwashita, Y.; Miyawaki, E.; Takeuchi, Y.; Tongu, H., Compact H^+ ECR Ion Source with Pulse Gas Valve, *AIP Conf. Proc.*, **2011-1,** [030011-1]-[030011-3] (2018).

Iwashita, Y.; Fuwa, Y.; Ishida, T.; Kino, K., Magnified Neutron Imaging with Modulating Permanent Magnet Sextupole Lens, *Proc. Int. Conf. Neutron Optics (NOP2017)*, **22,** [011008-1]-[011008-7] (2018).

Fuwa, Y.; Iwashita, Y., Performance Evaluation of a Klystron Beam Focusing System with Anisotropic Ferrite Magnet, *Prog. Theor. Exp. Phys.*, **2017-2,** [023G01-1]-[023G01-14] (2017).

Imajo, S.; Mishima, K.; Kitaguchi, M.; Iwashita, Y.; Yamada, N. L.; Hino, M.; Oda, T.; Ino, T.; Shimizu, H. M.; Yamashita, S.; Katayama, R., Pulsed Ultra-cold Neutron Production Using a Doppler Shifter at J-PARC, *Prog. Theor. Exp. Phys.*, **2016-1,** [013C02-1]-[013C02-22] (2016).

Fuwa, Y.; Iwashita, Y.; Tongu, H.; Inoue, S.; Hashida, M.; Sakabe, S.; Okamura, M.; Yamazaki, A., RF Synchronized Short Pulse Laser Ion Source, *Rev. Sci. Instrum.*, **87-2,** [02A911-1]-[02A911-4] (2016).

Kubo, T.; Iwashita, Y.; Saeki, T., Radio-frequency Electromagnetic Field and Vortex Penetration in Multilayered Superconductors, *Appl. Phys. Lett.*, **104,** 032603 (2014).

Evaluation of Superconducting Characteristic on the Multilayer Thin-Film Structure That Consists of NbN and Insulator Layer on Pure Nb Substrate

In recent years, it has been pointed out that the maximum accelerating gradient of a superconducting RF cavity can be pushed up by coating the inner surface of the cavity with a multilayer thin-film struture that consists of alternating insulating and superconducting layers. In this structure, the principal parameter that limits the performance of the cavity is the critical magnetic field or effective H_{C1} at which vortices start penetrating into the superconductor layer, and it is predicted to depend on the combination of the thicknesses of the layers. Hereafter, such multilayer structures on pure bulk Nb in superconducting state is referred to as S-I-S (Superconductor-Insulator-Superconductor) structure. The effective H_{C1} of a superconducting material can be evaluated by applying an AC magnetic field to the material with a small coil and detecting the induced third-harmonic signal at the coil. Hereafter, this method is called third harmonic voltage method.

For the third harmonic voltage method, an AC magnetic field at the angular frequency of 5 kHz is generated by a coil close to the superconducting sample and the third harmonic voltage $v_3(t) = V_3 \sin(3\omega t)$ induced in the coil is simultaneously measured, where ω is the angular frequency of a sinusoidal drive current, $I_0 \sin(\omega t)$ represents the current flowing through the coil, and V_3 is the amplitude of $v_3(t)$. If the temperature of a sample in the superconducting state is being raised while the amplitude of AC magnetic field H_0 is fixed, V_3 suddenly rises when H_0 exceeds the effective H_{C1} of the sample at a certain temperature. In the measurement performed at Kyoto University, H_0 is controlled by drive current I_0, and the temperature dependence of the effective H_{C1} is evaluated from the temperatures at moments when V_3/I_0 suddenly rises.

We have tested a multilayer sample that consist of NbN and SiO_2 coated on pure bulk Nb. The pure bulk Nb substrate of the sample is pretreated with the standard electropolishing recipe for bulk Nb cavity. The multilayer sample is prepared using DC magnetron sputtering technique (ULVAC, Inc.). This sample is a thin-film structure of 200-nm-thick NbN and 30-nm-thick SiO_2.

The temperature dependence of the measured effective H_{C1} of the sample is depicted in Figure 1. The horizontal and vertical axes represent the temperature and the measured effective H_{C1}, respectively. The measured values of H_{C1} of pure bulk Nb sample and the effective H_{C1} of NbN(200 nm)/SiO_2(30 nm)/Nb sample are represented by the open circles and black triangles, respectively. In general, the temperature dependence of H_{C1} satisfies the following equation:

$$F(T) = F(0) \times \left(1-\left(T/T_c\right)^2\right).$$

The red curve is the theoretical curve obtained from the function of $F(T)$ assuming $F(0)$ = 180 mT and T_c = 9.2 K, which is used for calibration. The green dashed curve is obtained by fitting data points of the sample in the region T <9.2 K to the function of $F(T)$. On the other hand, the blue one dot chain line is obtained by fitting data points of the sample in the region T >9.2 to the function $F(T)$ at which T_c was fixed at 13.8 K, a value obtained from the measurement result of the critical temperature of NbN film. At temperatures below around 9.2 K, S-I-S structure is formed because both pure bulk Nb and NbN film are in superconducting state. Thus, the effective H_{C1} of the whole NbN/SiO_2/Nb structure in the superconducting state is expressed by the green dashed curve. On the other hand, for temperatures greater than around 9.2 K, S-I-S structure does not hold. Thus, the blue one dot chain line corresponds to the effective H_{C1} of only NbN film. As a result of fitting, $F(0)$ and T_c are estimated as $(210 \pm 7) \times 10^{-3}$ and 9.21 ± 0.02 K, respectively for the green dashed curve, whereas $F(0)$ is determined as $(3.3 \pm 0.5) \times 10^{-3}$ for the blue one dot chain line. It is thus confirmed that $F(0)$ of NbN(200 nm)/SiO_2(30 nm)/Nb in the region of T <9.2 K is improved by 17 % compared to that of pure bulk Nb. The measurement result clearly showed that the effective H_{C1} of pure bulk Nb improved by using the multi-layer film coating of S-I-S structure.

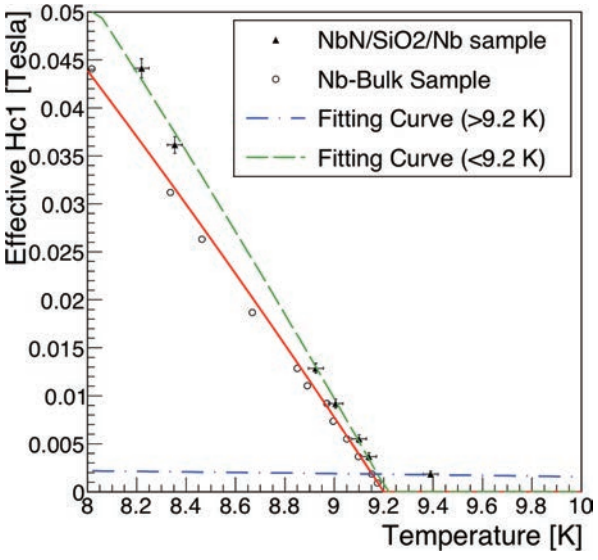

Figure 1. Comparison of measured effective H_{C1} between NbN(200 nm)/SiO_2(30 nm)/Nb and pure bulk Nb samples. The red curve represents $0.18 \times \left(1-\left(T/9.2\right)^2\right)$., which is used for calibration. The green broken line and the blue chain line are obtained by fitting data points of sample.